DOI: 10.7860/JCDR/2021/50888.15324

Original Article

Radiology Section

COVID-19 Associated Rhino-orbito-cerebral Mucormycosis: Clinical Profile and Imaging Spectrum

RITEMA MANGAL[1], PRATEEK SINGH GEHLOT[2], ANUJ BANG[3], ARUSHI KAUSHAL[4], RISHIKESH KOLARE[5]

ABSTRACT

Introduction: Rhino-orbito-cerebral mucormycosis is a fatal disease caused by saprophytic fungi seen almost exclusively in diabetic and immunocompromised patients.

Aim: To describe various imaging findings of mucormycosis, and to emphasise the importance of imaging in its diagnosis and management.

Materials and Methods: A retrospective, observational, single centre study was done including patients with clinical and microbiological evidence of rhino-orbito-cerebral mucormycosis, who had a history of Coronavirus Disease 2019 (COVID-19) infection and had undergone Computed Tomography (CT) and/or Magnetic Resonance Imaging (MRI) scan of the head, orbit, and paranasal sinuses during the period of one month from 1st-31st May 2021. The clinical and imaging data of 67 such cases were interpreted and analysed by two radiologists.

Results: The study included 67 patients out of which 44 were male and 23 were female, and the average age of patients was 49±13 years. During their treatment for COVID-19, 55 (82.08%) patients had a history of hospitalisation and administration of supplemental oxygen, all 67 (100%) patients had taken broad spectrum antibiotics, 56 (83.58%) patients had taken steroids, 20 (29.85%) patients previously had a history of diabetes with worsening of glycaemic control during COVID-19 infection, and 47 (70.15%) patients were diagnosed with new onset hyperglycaemia. On imaging i.e., on CT and/or MRI with or without contrast, the infection was found to primarily affect the sino-nasal region. There was unilateral or bilateral involvement of single or multiple paranasal sinuses in all 67 patients with involvement of nasal cavity in 42 patients. Maxillary sinus was the most common and consistently involved sinus seen in all 67 patients, followed by ethmoid sinus seen in 54 patients. Additionally, 56 patients had extra-sinus disease with spread along vessels, nerves, or via bone erosion. CT showed soft tissue thickening, oedema, and fat stranding with or without bone erosion as the predominant finding in involved areas, while MRI showed Short Tau Inversion Recovery (STIR) hyperintense soft tissue thickening and postcontrast enhancement as the main finding.

Conclusion: There is a complex interplay of various COVID-19 infection and treatment related factors that are responsible for increased susceptibility to mucormycosis infection. Imaging plays an important role in aiding the diagnosis, determining the extent and spread of infection, guiding the extent of the surgical intervention, and determining the prognosis of these patients. The contrast enhanced MRI along with plain CT should be the preferred choice of imaging.

Keywords: Coronavirus disease-2019, Invasive fungal infection, *Rhizopus*, Sinonasal disease

INTRODUCTION

The COVID-19 is a disease caused by a new coronavirus called Severe Acute Respiratory Syndrome Corona Virus 2 (SARS-CoV-2) [1,2]. It is a global public health crisis associated with substantial mortality and morbidity worldwide [3]. Since its outbreak in December 2019, the disease spectrum has expanded from respiratory infection to additionally include various multisystem problems and secondary infections. The second wave of COVID-19 in India specifically has been associated with a significant rise in the number of rhino-orbito-cerebral mucormycosis cases resulting in an epidemic like situation.

Rhino-orbito-cerebral mucormycosis is a disease caused by several genera of fungi of the class Zygomycetes and the family Mucoraceae [4]. The genera, in order of decreasing frequency, are *Rhizopus, Mucor*, and *Absidia. Rhizopus* accounts for 90% of cases of rhino-orbito-cerebral mucormycosis. Mucorales are ubiquitous throughout the environment, and humans are exposed to them on a regular basis [4]. The spores of the fungus are inhaled through the mouth and nose, but infection rarely occurs in a person with an intact immune response. However, an immunocompromised individual is unable to mount an adequate immune response against the inhaled spores resulting in germination and hyphae formation with infection most commonly affecting the sinuses and lungs. The immunomodulating and hyperglycaemic effects of COVID-19 infection, uncontrolled diabetes, immunosuppressive therapy, and prolonged hospitalisation with non invasive/invasive ventilation create an ideal milieu for contracting mucormycosis. Initially, there is hyphal invasion seen in the mucosa of paranasal sinuses and nasal cavity resulting in symptoms of nasal blockage, postnasal drip, dark blood-tinged or mucoid secretions, rhinorrhea, sinus tenderness, headache, malaise, and fever. It may remain confined to the sinuses or may infiltrate into surrounding soft tissue i.e., orbit, oral cavity, and brain by angioinvasion, bone erosion, or perineural spread resulting in a myriad of symptoms like facial and periorbital oedema or numbness, blurred vision, chemosis, proptosis, diplopia, corneal anaesthesia, ophthalmoplegia, altered mental status, seizures, paresis, and cranial nerve involvement, especially of those along the cavernous sinus. Clinically, black eschar, crusting, necrotic tissue is seen over the turbinates, septum, and palate [4].

Early recognition of this life threatening infection is the key to allow for optimal treatment and improved outcomes [5]. Delay of a week often doubles the 30-day mortality from 35-66% [6]. CT and MRI are invaluable tools that are complementary to clinical evaluation in assessing the extent of disease and diagnosis of complications [7].

The objective of this study was to describe in detail the CT/MRI findings of mucormycosis patients and their significance in early diagnosis and management.

MATERIALS AND METHODS

A retrospective, observational, single centre study, including 67 mucormycosis patients who had undergone CT/MRI during the

period of one month from 1st-31st May 2021, was carried out at the Department of Radiodiagnosis, RD Gardi Medical College, and CR Gardi hospital, Ujjain, Madhya Pradesh, India. The study was conducted in the month of June 2021 after the approval of the Institutional Ethical Committee (IEC) reference number-IEC-RDGMC 07/2021.

Inclusion criteria: Patients with proven mucormycosis who had a definite preceding history of COVID-19 infection and who had undergone CT and/or MRI of the brain, orbit, and paranasal sinuses. Authors defined proven mucormycosis as individuals with a clinically compatible disease and demonstration of fungi (broad ribbon-like aseptate hyphae) using KOH (Potassium Hydroxide) mount by direct microscopy. The history of prior COVID-19 infection by positive Reverse Trancriptase Polymerase Chain Reaction (RT-PCR) report was confirmed in all patients.

Exclusion criteria: Patients without proven mucormycosis or definite evidence of COVID-19 were excluded from the study.

Data Acquisition

Relevant clinical and microbiological information was collected by retrieving patient files from hospital archives. Their CT/MRI scans were retrieved from the archives of the Radiology department.

CT technique: GE 128 slice scanner (Optima 660) was used. Axial images including the brain, orbit, and paranasal sinuses were taken using 120 kV, variable mA, 0.625 mm slice thickness, and 40 mm collimation followed by MPR and postprocessing.

MR technique: GE 3T machine (Architect 3T) was used. T1-weighted (T1W), T2-weighted (T2W), Fluid Attenuated Inversion Recovery (FLAIR), Diffusion Weighted Imaging (DWI) and STIR images were obtained in various planes. Postcontrast T1Fatsat images were taken in axial and coronal planes after administration of 0.2 mL/kg (0.1 mmol/kg) of IV gadolinium. The parameters for various sequences were as follows:

T1W: TR 630 ms, TE 12.9 ms, slice 3 mm/1 mm space Field Of View (FOV) 15×14

T2W: TR 4744 ms, TE 151.3 ms, slice 5 mm/1.5 mm space, FOV 24×24

STIR: TR 4432 ms, TE 79.6 ms, slice 4 mm/0.4 mm FOV 20×20

DW: B1000 4.5 mm/1 mm space FOV 24×24

FLAIR: TR 12000, TE 143.4 slice 4.5 space 1 mm FOV 22×22

Contrast enhanced Fat Suppressed: T1W TR 611 TE 9.4, 3 mm/0.5 mm space. FOV 18×18.

Imaging interpretation: The CT and/or MRI images were reviewed by two radiologists, having four years and 15 years of experience in cross-sectional imaging. The final opinion regarding imaging characteristics, sites, the extent of involvement, and complications was made through consensus.

STATISTICAL ANALYSIS

Categorical variables were presented as frequency and percentage. The clinical and imaging data were analysed using Statistical Package for Social Sciences Program (SPSS), version 21.0.

RESULTS

The study group comprised a total of 67 patients. There were 44 males and 23 females with ages ranging from 12-100 years (mean age was 49±13 years). The majority of patients (n=60) were aged over 40 years. During their treatment for COVID-19, 55 (82.08%) patients had a history of hospitalisation and administration of supplemental oxygen, all 67 (100%) patients had taken broad spectrum antibiotics, 56 (83.58%) patients had taken steroids, 20 (29.85%) patients previously had a history of diabetes with worsening of glycaemic control during COVID-19 infection, and 47 (70.15%) patients were diagnosed with new-onset hyperglycaemia.

Imaging: Out of 67 patients, 23 patients underwent non contrast CT scan, 10 patients underwent non contrast MRI, 10 patients underwent contrast-enhanced MRI and 24 patients underwent both plain CT and non contrast or contrast-enhanced MRI.

Sino-nasal involvement: All patients showed primary involvement of paranasal sinuses. The involvement of sinuses was bilateral in 47 cases and unilateral in 20 cases. The maxillary sinus was the most common and consistently involved sinus seen in all 67 cases, followed by ethmoid sinus seen in 54 patients. The involvement pattern of the sinuses is mentioned in [Table/Fig-1].

Sinus involved	No. of patients
All sinuses	34
Maxillary+Ethmoid+Sphenoid	6
Maxillary+Ethmoid+Frontal	6
Maxillary+Ethmoid	8
Maxillary+Fontal	1
Maxillary+Sphenoid	3
Maxillary only	9

[Table/Fig-1]: Pattern of involvement of paranasal sinuses.

On both CT and MRI, there were varying degrees of mucosal thickening with intra-sinus secretions and debris. On CT scan, the intra-sinus contents were either isodense or heterogeneous with hyperdensities [Table/Fig-2a]. On MRI, the mucosal thickening was hypointense to isointense on the T1W sequence and hyperintense on the T2W sequence. In some cases, T2 hypointense thickening was also seen. The mucosal thickening showed three enhancement patterns on contrast-enhanced MRI: 1) homogenous enhancement; 2) peripheral enhancement with central non enhancement; and 3) non enhancement indicating necrosis [Table/Fig-2b]. The retained intra-sinus secretions were isointense on T1 with T2 variable signal without any postcontrast enhancement. Restricted diffusion was seen in some of the cases.

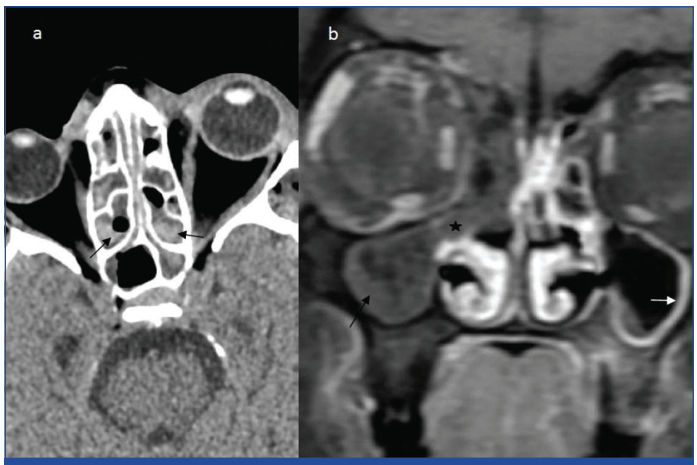

[Table/Fig-2a,b]: Axial CT image of a patient: (a) showing heterogeneous intra-sinus contents with central hyperdensity in bilateral ethmoid sinuses (black arrows). Coronal postcontrast T1FatSat image of another patient; (b) Showing non enhancing mucosal thickening along right maxillary sinus (black arrow) extending to osteomeatal region and right nasal cavity (black star) suggesting necrosis. On the left-side, however, mucosal enhancement is present (white arrow).

The involvement of the sinus wall and contiguous bones in form of erosions and permeative destruction on CT and bone marrow oedema on MRI was seen in 25 cases [Table/Fig-3].

Nasal cavity involvement was seen in 42 patients. Non specific mucosal thickening was the most common imaging finding. Hypertrophy/irregular mucosal thickening/destruction of turbinates was also seen [Table/Fig-4a]. Hypo or non enhancement of structures of the nasal cavity was an indicator of necrotic changes [Table/Fig-2b]. Seven patients had destruction of turbinates or septum or floor of the nasal cavity.

There was contiguous involvement of the nasopharynx in six cases seen as mucosal oedema and irregularity [Table/Fig-4b].

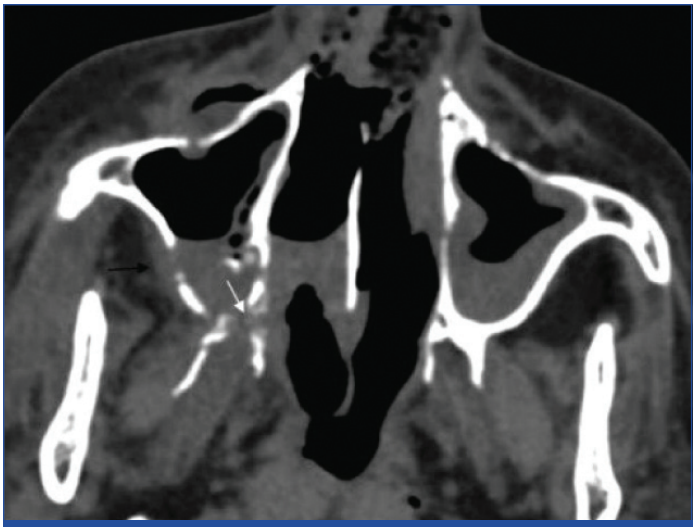

[Table/Fig-3]: Axial CT image of a patient showing infiltration in right retro-maxillary and pterygopalatine fossa (black arrow) with bone erosions seen in posterolateral wall of the maxillary sinus and pterygoid body (white arrow).

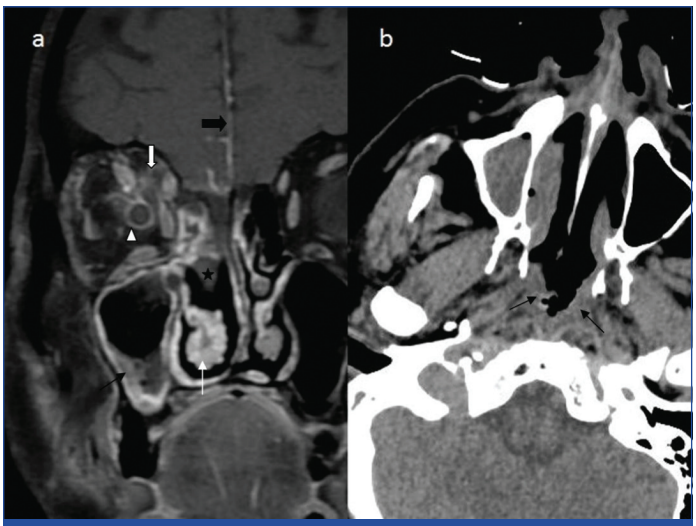

[Table/Fig-4a,b]: Coronal postcontrast T1FatSat image of a patient: (a) Showing involvement of right maxillary sinus and right nasal cavity (black arrow). Mucosal irregularity is seen along the right inferior turbinate (white arrow) with non enhancement and destruction of the right middle turbinate (black star). There is ill-defined infiltration seen in the extra and intraconal planes of the right orbit (white block arrow) with a prominent enhancement of the optic nerve sheath suggesting optic perineuritis (white arrowhead). Leptomeningeal enhancement was seen along the medial basifrontal region (black block arrow). Axial CT image of another patient; (b) Showing oedema and irregularity in the nasopharyngeal mucosa (black arrows).

Extra-sinus involvement: Amongst 67 patients evaluated, 11 patients had disease confined to the sino-nasal region while 56 patients had extra-sinus disease. The sites of extra-sinus involvement in decreasing order of frequency was as mentioned in [Table/Fig-5].

Site of extra-sinus disease	No. of patients (%)
Retromaxillary fat, masticator space, and pterygopalatine fossa	34 (50.74)
Orbit	33 (49.25)
Face (lid, premaxillary buccal fat, and upper lip)	19 (28.35)
Alveolus and oral cavity	15 (22.38)
Intracranial	10 (14.92)
Orbital apex/Cavernous sinus	11 (16.41)
Skull base	3 (4.47)

[Table/Fig-5]: Pattern of extra-sinus involvement.

The imaging findings in different extra-sinus sites were as below.

Retromaxillary fat, pterygopalatine fossa, and masticator space (across the postero-lateral wall of maxillary sinus): On CT, it was seen as variable soft tissue infiltration with effacement of fat planes and oedema along pterygoid muscles. On MRI, there was STIR hyperintense soft-tissue infiltration and/or ill-defined oedema-like signal with enhancement [Table/Fig-6].

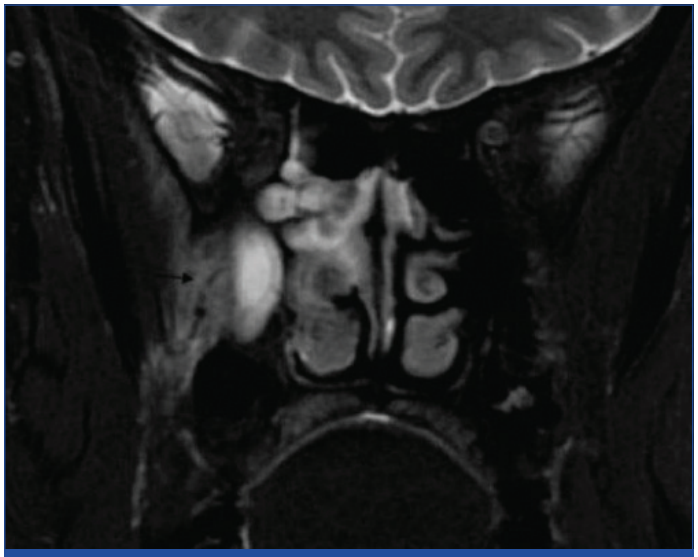

[Table/Fig-6]: Coronal STIR image of another patient showing hyperintense oedema-like signal in the retro-maxillary and masticator space (black arrow).

Orbit (along infra-orbital nerve/across the roof of maxillary sinus/ across lamina papyracea of ethmoid sinus/via nasolacrimal duct): The imaging findings were infiltrating soft tissue lesions or ill-defined fat stranding involving extraconal and less commonly intraconal fat planes with oedema and enlargement of the extraocular muscles [Table/Fig-4a,7a]. In one case, an extraconal abscess was seen. Changes of optic neuritis were seen on MRI as enlargement of the optic nerve, T2/STIR hyperintense signal, diffusion restriction, and enhancement [Table/Fig-7b]. The optic nerve involvement was seen extending to optic chiasma and ipsilateral optic radiation in one case. Perineuritis was seen as thickening and prominent enhancement of the optic nerve sheath [Table/Fig-4a]. Eye globe involvement/endophthalmitis was seen as altered shape, thickening of the orbital wall with prominent enhancement, and choroid membrane detachment [Table/Fig-7a,8a,b]. The pattern of orbital involvement is mentioned in [Table/Fig-9].

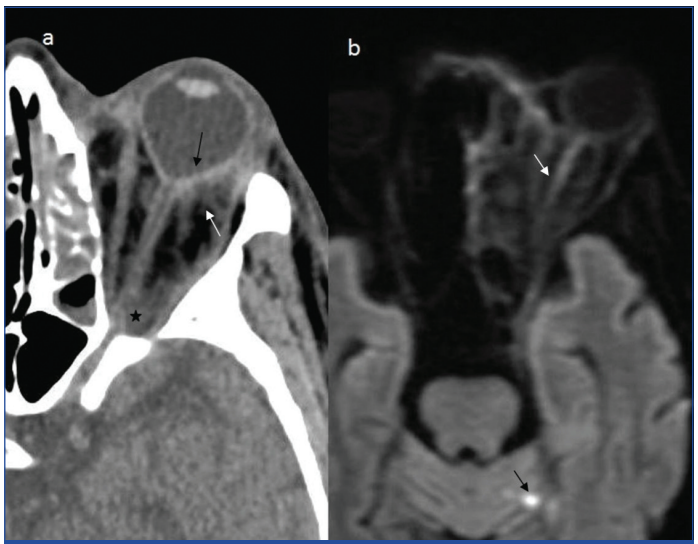

[Table/Fig-7a,b]: Axial CT image of a patient: (a) Showing ill-defined infiltrates and fat stranding in extra and intraconal fat planes of left orbit (white arrow) with altered shape of eyeball (black arrow) suggesting orbital cellulitis and endophthalmitis. Soft tissue infiltration is seen at the orbital apex (black star). Axial DWI image of another patient; (b) Showing diffusion restriction of left optic nerve, a sign of optic neuritis (white arrow). A small focus of diffusion restriction in cerebellum on left side is seen suggesting infarct (black arrow).

Fascial planes of lid, premaxillary buccal, and upper lip region (across the anterior wall of maxillary sinus): The various appearances on CT/MRI include oedema and fat stranding, nodular infiltration, and abscess formation [Table/Fig-10a,b].

[Table/Fig-8]: Axial FLAIR: (a) and Axial post contrast T1Fatsat images; (b) of the same patient showing altered shape of the left eyeball with thickening of ocular wall and choroid detachment suggesting endophthalmitis (black arrow). The extra-ocular muscles show hyperintense signal on FLAIR (white arrow) and hypo enhancement on post contrast images (white block arrow) suggesting impending infarction. On FLAIR image: (a) hyperintense perineural extension is seen along left trigeminal nerve in Meckel's cave extending upto nuclei in pons (black block arrow).

Compartment involved	No. of patients
Extra-conal only	10
Extra-conal+Extra-ocular muscles	3
Extra-conal+Extra-ocular muscles+Intra-conal	20
Associated optic neuritis	9
Associated optic perineuritis	4
Associated eye globe involvement	2

[Table/Fig-9]: Pattern of orbital involvement.

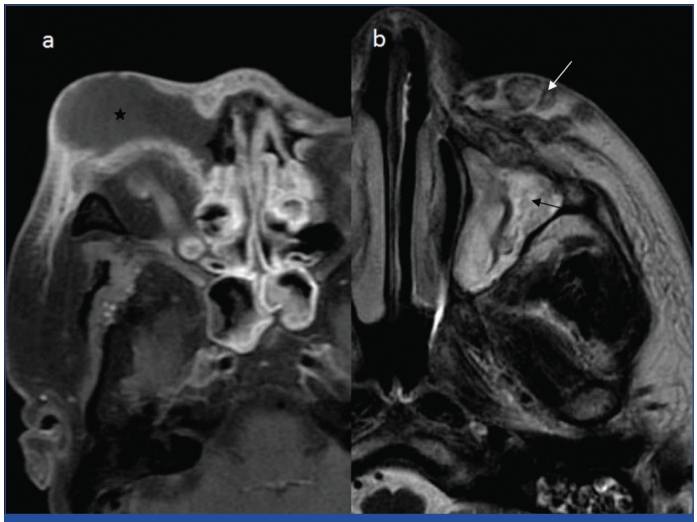

[Table/Fig-10]: Axial postcontrast T1Fatsat image of a patient (a) Showing bilateral ethmoid and sphenoid sinusitis with abscess in the right preseptal fat planes (black star). Axial T2 image of another patient (b) Showing heterogeneous intrasinus contents in left maxillary sinus with hypointensities within (black arrow). Nodular infiltrates were seen in the premaxillary fat planes (white arrow).

Oral cavity (across the floor of the maxillary sinus and nasal cavity): It was seen as marrow oedema on MRI and erosion of alveolus and hard palate on CT with thickening of the alveolar and palatal mucosa [Table/Fig-11a,b]. There was extensive destruction of the palate in two cases with communication between nasal and oral cavities.

Intracranial extension (into anterior cranial fossa across the wall of frontal sinus or cribriform plate/ into middle cranial fossa through pterygopalatine fossa via foramen rotundum/ perineural spread along 5th nerve to pons): It was seen as dural or leptomeningeal enhancement, extra-axial and/or intra-axial enhancing infiltrating granulomatous lesion, parenchymal oedema, cerebritis or abscess [Table/Fig-4a,12a-c]. Diffuse leptomeningitis with ependymitis was seen in one patient [Table/Fig-12d].

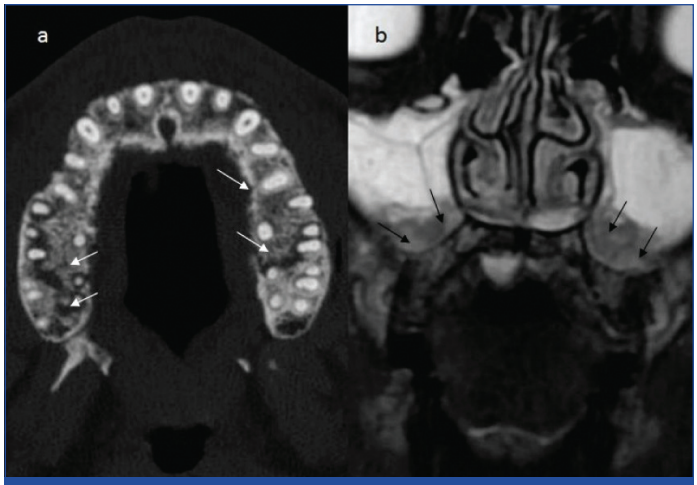

[Table/Fig-11]: Axial CT image of a patient: (a) Showing erosion and permeative destruction of maxillary alveolus (white arrows). Coronal STIR image of another patient; (b) Showing T2 hypointense lesions along the floor of the nasal cavity and bilateral maxillary sinuses infiltrating the palate and maxillary alveolus extending into palatal mucosa (black arrows).

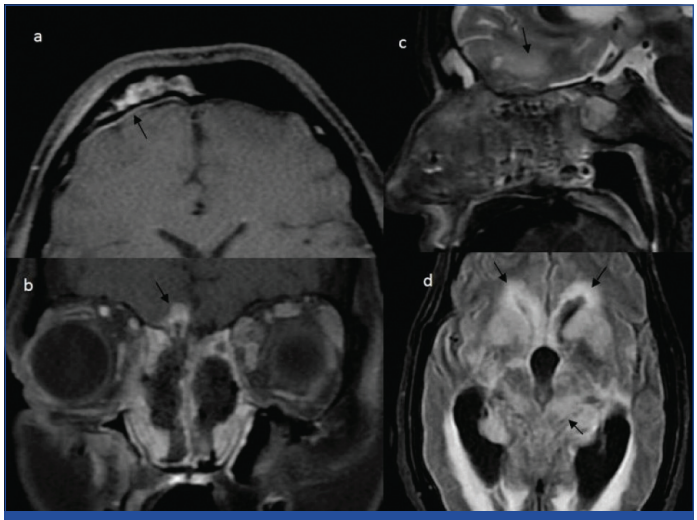

[Table/Fig-12]: Axial postcontrast T1FatSat image: a) Showing right frontal sinusitis and dural enhancement in right frontal region (black arrow). Coronal postcontrast T1FatSat; (b) and T2 sagittal images; (c) Showing infiltration across cribriform plate into basifrontal region (black arrows); (d) Axial FLAIR image showing diffuse leptomeningitis and ependymitis. Infiltrates are also seen along the basal cisterns (black arrows).

In some cases, perineural spread along the trigeminal nerve was seen via infratemporal fossa as diffusion restriction and enhancement of the nerve going to Gasserian ganglion in Meckel's cave and across the cisternal segment of nerve up to the nuclei in pons [Table/Fig-8a].

Infarcts and in one case intraparenchymal haemorrhage along arterial territories were also seen, likely due to mycotic thrombo-embolism [Table/Fig-7b].

Skull base involvement was seen in very few patients as T1 hypointense and STIR hyperintense marrow signal in bones with permeative erosion and destruction on CT.

Orbital apex and cavernous sinus (from orbit along optic nerve/ from pterygopalatine fossa along inferior orbital fissure): There was infiltrating soft tissue lesion at the orbital apex extending to the para sellar/ cavernous sinus region [Table/Fig-13a]. Non enhancement of the cavernous sinus suggesting thrombosis was seen in two cases [Table/Fig-13b,c]. Furthermore, there was involvement of ipsilateral internal carotid artery with thrombosis/vasculitis seen as an absence of flow void and hyperintense signal on MRI in two cases [Table/Fig-13d].

DISCUSSION

In this study, authors have discussed the correlation between the COVID-19 infection and rhino-orbito-cerebral mucormycosis. Authors have also focused on the imaging spectrum of mucormycosis with emphasis on its importance in diagnosis and management.

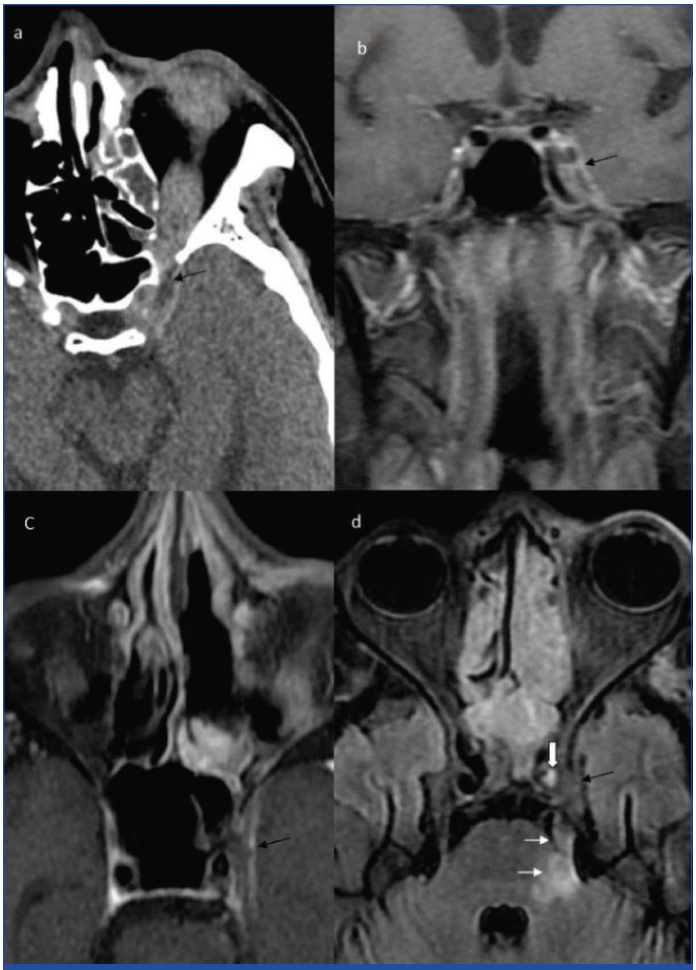

[Table/Fig-13]: Axial CT image: (a) Showing infiltration at the orbital apex extending into the cavernous sinus (black arrow). Coronal (b) and Axial postcontrast T1 FatSat images; (c) of a patient showing asymmetry and non enhancement of the left cavernous sinus suggesting thrombosis (black arrows). Axial FLAIR image of another patient; (d) Showing infiltration in left cavernous sinus (black arrow). Note the absence of flow void in the cavernous segment of the left internal carotid artery (white block arrow). Also, there is infiltration into Meckel's cave with perineural extension to the nuclei in pons (white arrows).

Singh AK et al., conducted a systematic review of literature on total of 101 patients to find out the characteristics of patients having mucormycosis and COVID-19 and concluded that an unholy trinity of diabetes, rampant use of corticosteroid in a background of COVID-19 appears to increase mucormycosis [8]. Sharma S et al., studied the association between COVID-19 and mucormycosis and concluded that uncontrolled diabetes and over-zealous use of steroids are two main factors aggravating the illness [9].

There is a complex interplay of factors that are responsible for mucormycosis in patients with a history of COVID-19 infection. The binding of SARS-CoV to the Angiotensin Converting Enzyme 2 (ACE2) receptors on pancreatic islets could potentially cause acute diabetes. In addition, SARS-CoV-2 might be associated with elevated amylase, lipase, and focal changes to the pancreas, raising the possibility of pancreatic injury [10]. This results in an acute deterioration of the glycaemic control during COVID-19 infection with resultant new-onset diabetes or increase in blood glucose levels and risk of ketoacidosis in patients with pre-existing type II diabetes. COVID-19 infection itself causes profound lymphopenia, disruption of epithelial-endothelial barrier, over-expression of inflammatory cytokines, and impaired cell-mediated immunity with a decreased (Cluster of Differentiation) CD4+ T and CD8+ T cells, markedly compromising the host immunity [9]. Additionally, the administration of steroids results in a neutrophilic leukocytosis with the impaired ability of leukocytes to migrate to the site of inflammation [11]. Steroids are also known to cause further lymphopenia (T more than B cells) and worsening of the hyperglycaemic state of the COVID-19 patients. An acidic, high-glucose environment with lowered immunity favours the growth of *Rhizopus* responsible for mucormycosis. In addition to this, patients who had a longer duration of hospital stays, who were admitted to intensive care units, and those who required invasive or non invasive ventilation due to Acute Respirtory Distress Syndrome (ARDS) were found to be more prone to develop a nosocomial fungal infection consistent with these theories and studies, all 67 of present study patients were found to have at least one of these predisposing factors or a combination of them.

The CT and MRI findings in the early stage, seen as variable density and intensity mucosal thickening and intra-sinus contents, are non specific and resemble the more mundane rhino-sinusitis. Middlebrooks EH et al., proposed a seven variable CT-based model to triage patients for acute invasive fungal sinusitis into a disease positive or negative category with a high degree of confidence. The variables included were periantral fat, bone dehiscence, orbital invasion, septal ulceration, pterygopalatine fossa, nasolacrimal duct, and lacrimal sac [12]. Safder S et al., and Taylor AM et al., described 'black turbinate sign' with focal non enhancement of mucosa and diffusion restriction on MRI as early MRI findings aiding the diagnosis of nasal mucormycosis [13,14]. Consistent with these studies, in this study also the initial findings were non specific. However, on CT scan, hyperdense intra-sinus contents, and on MRI, T2 hypointense signal of mucosal thickening and intra-sinus contents with diffusion restriction and non enhancement of mucosa were considered reliable findings for the diagnosis of fungal infection. Also, presence of bone erosions and infiltration in periantral planes on CT/MRI was highly indicative of invasive sinusitis.

Mondel P et al., and Therakathu J et al., described the spectrum of findings in rhinocerebral mucormycosis on CT and MRI and its role in assessing the extent of involvement and complications [7,15]. Hererra DA et al., described common radiographic patterns that may be useful in predicting the diagnosis of rhinocerebral mucormycosis and proposed that progressive and rapid involvement of the orbit, cavernous sinus, vascular structures, and intracranial contents is the usual evolution of this disease [16]. Mclean FM et al., described the perineural spread of mucormycosis with the involvement of cavernous sinus and internal carotid artery [17]. Present study also showed many of the similar imaging findings described previously with disease confined to sinonasal region seen in 11 patients and invasive rhino-sinusitis extending to one or multiple of the extra-sinus sites seen in 56 patients. Imaging aided in determining the sites of involvement, the viability of the involved tissue, and the extent of necrosis.

Groppo ER et al., described that MRI is more sensitive than CT in detecting early changes of acute fulminant invasive fungal sinusitis [18]. The multiplanar capabilities of MRI with its superior soft tissue depiction are helpful in delineating the anatomical extent of disease as well as its complications [2,15,16]. In our experience also, contrast-enhanced MRI provides more information than CT while CT is useful in picking up bone erosions, MR with contrast should be preferred over CT for the following reasons: 1) The T2 hypointensity and/or non enhancement of the sinonasal wall was seen as a sign highly suspicious of the disease; 2) The viability of tissue could be determined with non enhancement or hypoenhacement of sinonasal walls and extra-ocular muscles indicating impending infarction/necrosis (antifungal has a limited role in such cases and debridement is indicated); 3) Optic neuritis and perineuritis can be easily picked up with diffusion restriction, optic nerve or nerve sheath enhancement; 4) Subtle intracranial extension with only dural or leptomeningeal enhancement can be reliably diagnosed; 5) Perineural spread along with infraorbital nerve, optic nerve and trigeminal nerve can be picked up easily; 6) Involvement of bones can be identified in their early stages when only marrow oedema is seen; 7) Involvement of cavernous sinus and especially the internal carotid artery can be identified.

This study adds probably the largest series of rhino-orbito-cerebral mucormycosis in COVID-19 patients. This study should be helpful

in streamlining the imaging protocols for future studies on similar topics.

Limitation(s)

This study uses data from a single centre tertiary care hospital where most patients were referrals giving rise to selection bias with complicated patients coming to the institute for further management. There was no fixed imaging protocol for the study and so direct comparison of the diagnostic capabilities of CT and MRI was not made. Also, the impact of imaging findings on the final outcome of the patients was not evaluated because many of these patients were still undergoing the treatment while this study was done.

CONCLUSION(S)

There is a complex interplay of various COVID-19 infection and treatment-related factors namely deterioration of the glycaemic control, immunomodulation due to COVID-19 infection, diabetes, and steroid therapy, that are responsible for increased susceptibility to mucormycosis infection in patients with a history of COVID-19 infection. Imaging plays an important role in aiding the diagnosis and determining the extent and spread of this acute fulminant infection. In our experience, the contrast enhanced MRI with plain CT should be the preferred choice of imaging.

Acknowledgement

Authors would like to thank the Medical Director of R. D. Gardi Medical College, Dr. V.K. Mahadik, and the Dean, Dr. M.K. Rathore for granting us permission to conduct and publish this study.

REFERENCES

[1] World Health Organization. Coronavirus disease(COVID-19). https://www.who.int/health-topics/coronavirus#tab=tab_1. Accessed 12 July 2021.
[2] Awal SS, Biswas SS, Awal SK. Rhino-orbital mucormycosis in COVID-19 patients-a new threat? Egyptian Journal of Radiology and Nuclear Medicine. 2021;52(1):01-06.
[3] Bayram N, Ozsaygılı C, Sav H, Tekin Y, Gundogan M, Pangal E, et al. Susceptibility of severe COVID-19 patients to rhino-orbital mucormycosis fungal infection in different clinical manifestations. Jpn J Ophthalmol. 2021:65(4):515-25.
[4] Peter M. Som, Hugh D. Curtin. Head and Neck Imaging. 5th ed. Missouri: Elsevier publishing; 2011. Chapter 3: Inflammatory Diseases of the Sinonasal Cavities; P167-251.
[5] Nehara HR, Puri I, Singhal V, Sunil IH, Bishnoi BR, Sirohi P. Rhinocerebral mucormycosis in COVID-19 patient with diabetes a deadly trio: Case series from the north-western part of India. Indian J Med Microbiol. 2021;39(3):380-83.
[6] Maini A, Tomar G, Khanna D, Kini Y, Mehta H, Bhagyasree V. Sino-orbital mucormycosis in a COVID-19 patient: A case report. International Journal of Surgery Case Reports. 2021;82:105957.
[7] Mondel P, Udare A, Raut A. CT & MRI Imaging features of Rhinocerebralmucormycosis. European Congress of Radiology. 2012.
[8] Singh AK, Singh R, Joshi SR, Misra A. Mucormycosis in COVID-19: A systematic review of cases reported worldwide and in India. Diabetes & Metabolic Syndrome: Clinical Research & Reviews. 2021;15(4);102146.
[9] Sharma S, Grover M, Bhargava S, Samdani S, Kataria T. Post coronavirus disease mucormycosis: A deadly addition to the pandemic spectrum. J Laryngol Otol. 2021:135(5):442-47.
[10] Chee YJ, Tan SK, Yeoh E. Dissecting the interaction between COVID-19 and diabetes mellitus. Journal of Diabetes Investigation. 2020;11(5):1104-14.
[11] Saldanha M, Reddy R, Vincent MJ. Paranasal mucormycosis in COVID-19 patient. Indian J Otolaryngol Head Neck Surg. 2021:01-04.
[12] Middlebrooks EH, Frost CJ, De Jesus RO, Massini TC, Schmalfuss IM, Mancuso AA. Acute invasive fungal rhinosinusitis: A comprehensive update of CT findings and design of an effective diagnostic imaging model. American Journal of Neuroradiology. 2015;36(8):1529-35.
[13] Safder S, Carpenter JS, Roberts TD, Bailey N. The "black turbinate" sign: An early MR imaging finding of nasal mucormycosis. American Journal of Neuroradiology. 2010;31(4):771-74.
[14] Taylor AM, Vasan K, Wong EH, Singh N, Smith M, Riffat F, et al. Black turbinate sign: MRI finding in acute invasive fungal sinusitis. Otolaryngology Case Reports. 2020;17:100222.
[15] Therakathu J, Prabhu S, Irodi A, Sudhakar SV, Yadav VK, Rupa V. Imaging features of rhinocerebral mucormycosis: A study of 43 patients. The Egyptian Journal of Radiology and Nuclear Medicine. 2018;49(2):447-52.
[16] Herrera DA, Dublin AB, Ormsby EL, Aminpour S, Howell LP. Imaging findings of rhinocerebral mucormycosis. Skull Base. 2009;19(2):117.
[17] McLean FM, Ginsberg LE, Stanton CA. Perineural spread of rhinocerebral mucormycosis. American Journal of Neuroradiology. 1996;17(1):114-16.
[18] Groppo ER, El-Sayed IH, Aiken AH, Glastonbury CM. Computed tomography and magnetic resonance imaging characteristics of acute invasive fungal sinusitis. Archives of Otolaryngology-Head & Neck Surgery. 2011;137(10):1005-10.

PARTICULARS OF CONTRIBUTORS:
1. Assistant Professor, Department of Radiodiagnosis, R.D. Gardi Medical College, Ujain, Madhya Pradesh, India.
2. Associate Professor, Department of Radiodiagnosis, R.D. Gardi Medical College, Ujain, Madhya Pradesh, India.
3. Postgraduate Student, Department of Radiodiagnosis, R.D. Gardi Medical College, Ujain, Madhya Pradesh, India.
4. Postgraduate Student, Department of Radiodiagnosis, R.D. Gardi Medical College, Ujain, Madhya Pradesh, India.
5. Postgraduate Student, Department of Radiodiagnosis, R.D. Gardi Medical College, Ujain, Madhya Pradesh, India.

NAME, ADDRESS, E-MAIL ID OF THE CORRESPONDING AUTHOR:
Dr. Prateek Singh Gehlot,
B-5/18, R.D. Gardi Medical College, Ujain-456001, Madhya Pradesh, India.
E-mail: prateekgehlot@yahoo.com

PLAGIARISM CHECKING METHODS: [Jain H et al.]
- Plagiarism X-checker: Jun 21, 2021
- Manual Googling: Aug 06, 2021
- iThenticate Software: Aug 17, 2021 (12%)

ETYMOLOGY: Author Origin

AUTHOR DECLARATION:
- Financial or Other Competing Interests: None
- Was Ethics Committee Approval obtained for this study? Yes
- Was informed consent obtained from the subjects involved in the study? No
- For any images presented appropriate consent has been obtained from the subjects. No

Date of Submission: **Jun 14, 2021**
Date of Peer Review: **Jul 06, 2021**
Date of Acceptance: **Aug 12, 2021**
Date of Publishing: **Sep 01, 2021**